Research Square

Preprints are preliminary reports that have not undergone peer review.
They should not be considered conclusive, used to inform clinical practice,
or referenced by the media as validated information.

Irradiated Graphite Decontamination: 14 C and 3 H Release – A Steam-Assisted Thermal Treatment Approach

Lorie Meunier

l.meunier@th-mannheim.de

Technische Hochschule Mannheim

Niklas Heiß

Technische Hochschule Mannheim

Lotte Lens

Technische Hochschule Mannheim

Bako Abdolla

Technische Hochschule Mannheim

Eldhose Varkey

TU Berlin

Ulrich W. Scherer

Technische Hochschule Mannheim

Research Article

Keywords: thermal treatment, decontamination, irradiated graphite, pure beta-emitters radionuclides

Posted Date: June 12th, 2026

DOI: https://doi.org/10.21203/rs.3.rs-9804519/v1

License: This work is licensed under a Creative Commons Attribution 4.0 International License.
Read Full License

Additional Declarations: No competing interests reported.

Irradiated Graphite Decontamination: ^{14}C and ^{3}H Release – A Steam-Assisted Thermal Treatment Approach

Names of the authors: Lorie Meunier [1,2], Niklas Heiß [1,2], Lotte Lens [1,3], Bako Abdolla [1], Eldhose Varkey [4], Ulrich W. Scherer[1]
Title: Irradiated Graphite Decontamination: ^{14}C and ^{3}H Release – A Steam-Assisted Thermal Treatment Approach

Affiliation(s) and address(es) of the author(s): [1]Technische Hochschule Mannheim, Paul-Wittsack-Straße 10, Mannheim, 68163, Germany

[2]Department of Chemistry – TRIGA Site, Johannes Gutenberg-Universität Mainz, Fritz-Strassmann-Weg 2, Mainz, 55128, Germany
[3]Current adress : Safetec GmbH, Dischingerstraße 8, Heidelberg, 69123, Germany
[4]TU Berlin, Staudingerweg 18, Berlin, 10623, Germany
E-mail address of the corresponding author: l.meunier@th-mannheim.de

Corresponding author: Lorie Meunier

Funding : this project was funded by the Federal Ministry of Research, Technology and Space (BMFTR) of Germany, under grant number 15S9442

Irradiated Graphite Decontamination: ^{14}C and ^{3}H Release – A Steam-Assisted Thermal Treatment Approach

Lorie Meunier [1,2], Niklas Heiß [1,2], Lotte Lens [1,3], Bako Abdolla [1], Eldhose Varkey [4], Ulrich W. Scherer[1]

[1]Technische Hochschule Mannheim, Paul-Wittsack-Straße 10, Mannheim, 68163, Germany

[2]Department of Chemistry – TRIGA Site, Johannes Gutenberg-Universität Mainz, Fritz-Strassmann-Weg 2, Mainz, 55128, Germany
[3]Current adress : Safetec GmbH, Dischingerstraße 8, Heidelberg, 69123, Germany
[4]TU Berlin, Staudingerweg 18, Berlin, 10623, Germany

Abstract
Germany faces major challenges in disposing of irradiated nuclear graphite due to limited radionuclide inventory data and strict regulatory limits, particularly for ^{14}C. This study investigates an assisted steam thermal treatment to selectively remove volatile radionuclides (^{14}C and ^{3}H) from irradiated graphite while preserving the bulk material. Experiments on irradiated graphite from the FRJ-2 and TRIGA Mainz reactors were performed to study the effects of temperature, treatment duration, and humidity. Under optimized conditions, more than 85% of both radionuclides were removed, demonstrating the potential of high-temperature steam treatment to reduce radionuclide inventories and improve radioactive waste management.

Keywords: thermal treatment, decontamination, irradiated graphite, pure beta-emitters radionuclides

1. Introduction

Graphite is a material widely used in nuclear reactors due to its good physical and mechanical properties. It can be used as a moderator, reflector and construction material. The extensive use of graphite in nuclear technology has resulted in the accumulation of up to 250,000 t of irradiated graphite (i-graphite) worldwide, of which approximately 2,000 t originate from Germany's research reactors and the high-temperature reactor THTR (Thorium-Hochtemperatur-Reaktor) [1;2]. During reactor operation, the graphite and its impurities are exposed to neutron flux and are activated. This results in the formation of different radionuclides including the pure beta emitters: ^{14}C, ^{3}H and ^{36}Cl, as well as gamma-emitting radionuclides such as: ^{60}Co, ^{133}Ba, ^{152}Eu and ^{154}Eu. Irradiated graphite is therefore considered as low- and intermediate-level waste and must be disposed of properly [2].

However, problems arise when considering its final disposal. In Germany, the Konrad mine is designated as the final repository for low- and intermediate-level waste [2;3]. Strict regulatory limits are imposed on the maximum allowable activity of certain radionuclides such as ^{14}C and ^{3}H. Current estimates, based on activity inventories and assumed release behavior under an accident scenario, suggest that the disposal of irradiated graphite from the two German high-temperature reactors (Arbeitsgemeinschaft Versuchsreaktor (AVR) and Thorium-Hochtemperatur-Reaktor (THTR-300)) alone would consume roughly 90 % of the permissible

^{14}C inventory in the Konrad repository, leaving only a limited space for the other ^{14}C-containing wastes coming from industry, research and medicine [1;2]. Moreover, ^{14}C and ^{3}H are of particular concern due to their high expected volatility and, in the case of ^{14}C, its long half-life. As a result, their potential release into the environment represents a significant environmental risk.

An initial estimation of the radionuclide inventory can be obtained by using Monte Carlo simulations [4]. These approaches provide a first approximation of the expected radionuclide distribution; however, their accuracy is limited by the accuracy of the assumptions and the often-incomplete information on historical reactor materials. Differences in production methods, impurities, and trace element contents led to various graphite qualities, even within the same reactor. Moreover, the position of each graphite component relative to the reactor core and the corresponding neutron flux, combined with its individual irradiation history, strongly influences the types and amounts of radionuclides formed during operation. Therefore, experimental validation becomes crucial to confirm the model-based predictions and reduce the uncertainties. The experimental validation includes, in particular, characterization analyses to determine the radionuclide inventory and volatility studies that quantify the behavior of radionuclides mobilizable under repository-relevant conditions.

The i-GraDe (irradiated Graphite Decontamination) project was established to address these challenges. Its first objective is to develop an experimental way of characterizing i-graphite [5], and its second goal is to develop effective decontamination processes. This second part not only opens the possibility of selective removal of volatile radionuclides like ^{14}C and ^{3}H but also the possibility of reusing the treated graphite in technical applications, such as in small modular reactors (SMRs). The approach to decontaminate i-graphite allows for retaining the volatile radionuclides in repository stable forms separated from the i-graphite. As a consequence, some fraction of the i-graphite may be released after decontamination, some other fraction having lost the volatile species may better comply with the Konrad repository acceptance criteria. Among the potential strategies, thermal treatment has emerged as a particularly promising approach and represents the focus of this work. The irradiated graphite sample is subjected to high temperatures (1000 – 1500 °C) under controlled, weakly oxidative conditions, employing water vapor as the reactive medium. This process enables the selective removal of volatile radionuclides, most notably ^{14}C and ^{3}H, from the near-surface region of the graphite matrix. The methodology is based on earlier investigations carried out by one of the authors (UWS) at FH Aachen in cooperation with Forschungszentrum Jülich [1;6;7]. In the present study, it is further advanced using a high-temperature furnace capable of reaching higher temperatures and thus improving the potential release fraction of the different radionuclides. Different process variables are thoroughly tested such as the temperature and duration of treatment as well as the relative humidity, using i-graphite samples coming from different origins (FRJ-2 and TRIGA Mainz) to optimize the release of the pure beta-emitters ^{14}C and ^{3}H.

2. Material and methods

2.1. Irradiated graphite samples

2.1.1. Sample origins

Different samples were used for the thermal treatment and decontamination of the pure beta-emitters. They have two different origins: the TRIGA Mainz reactor at Johannes Gutenberg University Mainz and the FRJ-2 (Forschungszentrum Jülich). The FRJ-2 samples originate from five different sections of one singular 6-inch vertical drill (6VGR) core from the

graphite channel having about 12 cm of height each. Each section is named from 1 to 5, with section 1 being the closest to the reactor core and therefore exposed to the highest neutron flux and section 5 being the farthest away. The research reactor was permanently shut down in 2006. Samples of each section are available in fragments, ranging from a few mg to a few g. The used sample from the TRIGA Mainz consists of a square plate of 10 by 10 cm and is 1 cm thick. It was part of a graphite element, placed in the central position of the reactor's thermal column until 2005. For the thermal treatment, the TRIGA sample was cut into smaller rectangular pieces to reach a mass of around 75 mg and a size of about (0.5 x 0.6 x 1.0) cm. The FRJ-2 samples consist of small fragments of i-graphite of around 75 mg as well, with irregular geometry.

2.1.2. Reaction of irradiated graphite under oxidative conditions

During reactor operation, both the graphite matrix and its inherent impurities can undergo neutron activation, resulting in the formation of various radionuclides. Previous studies have shown that among these, ^{3}H and ^{14}C constitute major contributors to the overall activity of irradiated graphite [4]. For this reason, the present paper focuses exclusively on the release behavior of these two pure beta-emitters. To do so, thermal treatment is performed under inert gas and water-vapor atmospheres. Understanding the chemical processes that graphite undergoes under such conditions, particularly the temperature-dependent oxidation and gas–solid reactions, is essential to correctly interpret the release mechanisms. In addition, the relevant reactions involving carbon, hydrogen, and oxygen species must be considered to clarify how ^{3}H and ^{14}C are released during thermal treatment.

The thermally induced release of ^{3}H and ^{14}C is directly linked to the reactivity of graphite with oxidizing agents such as water vapor. This reactivity is strongly dependent on temperature and is influenced by factors such as material structure, sample size, porosity, and chemical purity [8]. The interaction of graphite with water vapor can be categorized into three temperature-dependent reactivity regimes, each distinguished by specific reaction mechanisms and spatial characteristics [6;9;10]:

Chemical regime (25 °C – 850 °C):

In the low-temperature regime (T < 850 °C), the oxidation of graphite is predominantly governed by chemical reaction kinetics. The high activation energy associated with the process limits the overall reaction rate, despite the oxidizing gas being able to diffuse readily across the graphite surface. Because this energy barrier significantly restricts reactivity, the gas concentration at the surface remains effectively constant, and the chemical reaction itself becomes the rate-controlling step. Under these conditions, oxidation occurs uniformly within the graphite pore network, resulting in more severe degradation of the material's mechanical integrity.

In-pore diffusion-controlled regime (850 °C – 1350 °C):

At elevated temperatures (850 °C – 1350 °C), oxidizing gases can penetrate more deeply into the graphite pore network, increasing the accessible reactive surface volume and thereby enhancing the overall oxidation rate. In this regime, the rate-controlling mechanism shifts from surface reaction kinetics to mass transport, dominated by diffusion within the pores. As the temperature rises further, the consumption of oxidizing gases inside the pore structure becomes increasingly significant, reducing the effective oxidation depth as fewer reactive species reach the inner regions of the material. This occurs because the temperature dependence of the chemical reaction rate is considerably stronger than that of in-pore gas diffusion, leading to the formation of a concentration gradient within the carbon matrix and a corresponding gradient in local burn-off (oxidation degree).

For isothermal, integral measurements, the oxidation rate initially increases with surface-related burn-off until reaching a plateau. While in idealized homogeneous carbon materials such behavior can be modeled using Fick's second law of diffusion combined with the reaction rate from Regime I, the heterogeneous nature of graphite, composed of graphitized filler and ungraphitized (coked) binder, limits the applicability of a simple effective diffusion coefficient. Consequently, even in relatively homogeneous nuclear graphite, predictions based on effective diffusion models may deviate from experimental observations [8;9;10]

Mass transfer-controlled regime (>1250 – 1450 °C, depending on graphite purity):

At very high temperatures, the oxidation of graphite is limited by the oxygen transfer rate from the gas phase to the exposed surface. Under these conditions, gas molecules are unable to diffuse into the bulk material and react exclusively at the external surface. This leads to fast corrosion of exposed surfaces, dimensional and shape changes. Consequently, mass transfer governs the overall oxidation rate and acts as the rate-limiting step. Although an analogy between mass and heat transfer is generally valid, the chemical kinetics of the carbon–oxygen reaction cannot be neglected at elevated temperatures. As temperature increases, carbon monoxide (CO) becomes the predominant oxidation product, being thermodynamically favored over carbon dioxide (CO_2). A secondary gas-phase reaction between CO and O_2 within the boundary layer near the graphite surface may generate CO_2. Since CO_2 also acts as an oxidizing agent for graphite, its formation in the boundary layer can initiate an additional oxidation pathway. This process further accelerates graphite corrosion, exceeding predictions based solely on mass transfer considerations [8;9].

As explained, the oxidation behavior of graphite is governed by several factors, including temperature, the nature of the oxidizing species, and the size and morphology of the sample. Among the various oxidants, water vapor is of particular interest, as it exhibits a distinct reaction pathway with graphite at elevated temperatures. Since the present study employs water vapor as the oxidizing medium, particular emphasis is placed on understanding the graphite–steam interaction. The following section describes in detail the mechanisms involved in this reaction.

When graphite is in contact with water vapor it reacts from about 800–900 °C [6;7] in the so-called water–gas reaction, which is of particular interest in thermal decontamination processes:

$$C(s) + H_2O(g) \rightleftharpoons CO(g) + H_2(g) \quad (1)$$

This reaction typically occurs in the second zone, the diffusion-controlled one, where the reaction gas can penetrate the pore structure of the graphite. It promotes the release of ^{14}C bound in the material in the form of CO and is therefore closely linked to the mobilization mechanism during steam reforming. The CO formed can, at temperatures below 400 °C, further react with water vapor to form CO_2 and hydrogen via the water–gas shift reaction:

$$CO(g) + H_2O(g) \rightleftharpoons CO_2(g) + H_2(g) \quad (2)$$

Other reactions might occur but with a lower probability, such as:

$$C(s) + CO_2(g) \rightleftharpoons 2\ CO(g) \quad (3)$$

This equilibrium is the Boudouard equilibrium. The equilibrium is temperature-dependent: at higher temperatures, the formation of CO is favored, while at lower temperatures, the formation of CO_2 is favored. Another reaction might be the formation of methane:

$$C(s) + 2H_2(g) \rightleftharpoons CH_4(g) \quad (4)$$

The radionuclides being in volatile chemical forms are trapped in a system of wash bottles filled with nitric acid and sodium hydroxide, which allow selective trapping of volatile ^{14}C and ^{3}H. The ^{14}C-containing reaction gases are catalytically converted to CO_2, which can be retained in the solution from the exhaust gas stream using NaOH:

$$CO_2 + 2\ NaOH \rightleftharpoons Na_2CO_3 + H_2O \quad (5)$$

In addition to CO_2, tritium may also be released during oxidation, predominantly in the form of tritiated water (HTO). Chemically, HTO is almost indistinguishable from ordinary water vapor and cannot be directly separated by chemical means. However, it can be effectively captured through physical absorption in a suitable liquid medium. For this purpose, an aqueous solution of nitric acid (HNO_3) is commonly employed. After absorption, tritium remains in the liquid phase as HTO. This process can be represented as:

$$HT + H_2O \rightleftharpoons HTO + H_2 \quad (6)$$

2.2. Characterization

High-temperature thermal treatment of i-graphite in water vapor induces partial oxidation and subsequent mass loss, calculated via pre- and post-treatment weighing. Minimizing this loss is desirable for recycling purposes; however, it is less critical when the main goal is purging volatile radionuclide fractions. Ultimately, the effectiveness of the treatment is assessed by measuring the release of 3H and 14C is measured. This evaluation requires characterization of the sample both before and after thermal treatment. A brief overview of the characterization is provided in the following section, while a detailed description of the ^{3}H and ^{14}C characterization can be found in Heiß et al.[5].

Since the radionuclides ^{3}H and ^{14}C are pure β-emitters, they are measured by liquid scintillation counting (LSC). However, this technique requires a destructive sample preparation using an oxidizer (OX-600 Oxidizer, Hidex). The oxidization step involves oxidizing the powderized graphite samples in a continuous stream of oxygen to convert the ^{3}H and ^{14}C into $^{14}CO_2$ and HTO and subsequently capturing the gases in suitable solutions (Oxidizer 600 OX Radiocarbon and Oxidizer 600 OX-Tritium). The ^{3}H and ^{14}C are selectively bound in different vials, allowing the direct measurement of the cocktail solutions using the LSC (SL-600, Hidex). Specific activities and associated uncertainties are calculated in accordance with DIN ISO 11929 [11].

To evaluate the release fraction of ^{3}H in the TRIGA and FRJ-2 i-graphite samples, a pre- and post-treatment characterization step was carried out. This step was performed differently according to the sample origin due to its geometry. For the TRIGA sample, sixteen evenly distributed spots across the square plate were drilled to collect powder, which was then combusted in the oxidizer. The material used for the thermal treatment was taken from areas close to these drilling points. Consequently, it was assumed that the specific activity of the sample subjected to thermal treatment corresponded to that of the nearest characterized point. Following the treatment, an additional drilling was performed at the center of the sample to obtain sufficient material for three combustion tests, ensuring representative results. To characterize the FRJ-2 sample, three fragments of the same section, each with a similar size, were oxidized. The resulting specific activity was averaged and used as a reference value for samples from this section. The same procedure was performed for all 5 sections. After treatment, the complete sample was milled down and homogenized to obtain enough material for three oxidizations while ensuring representative results.

To obtain the radionuclide release data described above, the sample must undergo the thermal treatment process. The experimental system developed for this purpose is presented in the following section.

2.3. Thermal treatment

2.3.1. High temperature oven

• System setup

A system has been designed for the thermal treatment of i-graphite samples with the goal of releasing volatile radionuclides and capturing them in a more stable form in suitable solutions. The experimental setup was developed based on the experimental setup used by Krauss et al. [6]. The current system is able to reach higher temperatures with more accuracy [12]. Additionally, the system was setup to allow precise and flexible adjustment of all process parameters, such as humidity proportion in the gas, temperature, gas flow, and treatment duration. The complete system is presented in Figure 1.

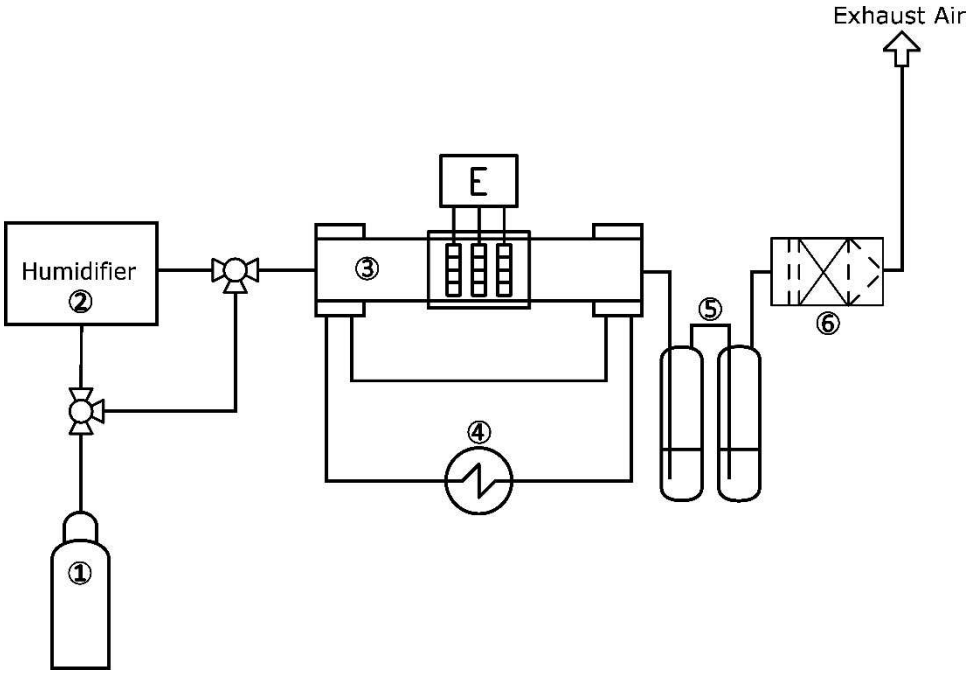

Figure 1: Complete system of thermal treatment with an inlet gas (1), which can be humidified with water vapor via a humidity generator (2) or fed directly into the high-temperature furnace (3). The flanges are kept temperature-stable by a cooling system (4). The resulting reaction gases pass through two wash bottles (HNO_3 and NaOH) (5) to bind gaseous radionuclides and then through an activated carbon filter (6) to retain any residual substances. The purified gas stream is finally safely discharged into the exhaust system [13].

The gas supply is provided via gas cylinders containing argon (5.0) (1). Depending on the desired humidity level in the system, the gas can either be directed through a humidifier or bypassed. The humidity system used is the Flexi Wet 200 from Setaram. The gas temperature can reach up to 50 ± 0.1 °C, with a relative humidity ranging from 0 to 95 ± 0.3 %. The maximum flow rate in humidified mode is 12 $L.h^{-1}$. If the gas bypasses the humidifier, the maximum flow rate is 500 $L.h^{-1}$. In the present work, the flow rate is fixed at 12 $L.h^{-1}$ for every experiment.

The i-graphite samples can be inserted and removed using quick-release flanges, allowing for rapid exchange inside the furnace (3). The experiment is conducted using a high-temperature furnace from Nabertherm, capable of reaching a maximum temperature of 1600 °C. The furnace is equipped with six SiC rod heating elements to ensure a homogeneous temperature distribution. Inside the furnace is an Al_2O_3 (aluminum oxide) tube with dimensions of 820 × 430 × 580 mm, an outer diameter of 80 mm, and a material purity classified as C799 (99.7 %).

To avoid thermomechanical stresses, a recommended heating rate of 300 $K.h^{-1}$ is applied. Cooling is conducted at a comparable rate of approximately 300 $K.h^{-1}$, ensuring uniform thermal relief of the furnace components. Temperature is measured and regulated using a centrally positioned thermocouple connected to a control unit. The flanges on both sides of the furnace are equipped with a water-cooling system (4), which limits the thermal stress on the installed sealing systems. At the exit of the furnace, the gas stream is cooled down to around 50°C by ambient air before reaching the wash bottles. Two wash bottles (5) are connected in series. The first bottle contains a solution of 0.1 M HNO_3 to bind HTO, and the second contains a solution of 4 M NaOH to capture $^{14}CO_2$.

For additional safety, an activated carbon filter (6) is installed downstream of the wash bottles. It serves to adsorb volatile compounds not captured in the washing liquid and acts as a secondary retention stage to minimize potential emissions. With the safety components in place, the next step involved validating the complete system to confirm its operational performance prior to running systematic experiments.

- System validation

The complete system was tested and validated by Abdolla et al [13]. Following this validation phase, preliminary experiments were carried out in this study to compare the release fractions of ^{3}H and ^{14}C obtained with the new setup to those previously measured using the system developed by Krauss et al. [6]. They identified optimal release conditions at 1000 °C with a relative humidity of 28.8 %. These parameters were therefore applied in the present work and tested for treatment durations of 2 h and 4 h. The results obtained with both systems for these treatment times are presented in Table 1.

Table 1: Comparison of ^{3}H and ^{14}C release fractions measured by of Krauss et al. [6] and from the current study, under formally identical treatment parameters (1000 °C, 28.8 % Relative humidity (RH), 2 h/4 h). Note that uncertainties are available only for the current study and are listed in percent.

	Release fraction of ^{3}H (%)		Release fraction of ^{14}C (%)	
	Current study	Krauss et al. [6]	Current study	Krauss et al. [6]
1000 °C, 2 h, 28.8 % RH	54 ± 4	37	24 ± 7	6
1000 °C, 4 h, 28.8 % RH	61 ± 6	72	36 ± 7	15

Both the ^{3}H and ^{14}C release fractions obtained in this study are higher than those reported by Krauss et al. for a 2 h treatment. For a 4 h treatment, only the release of ^{14}C is higher. Several factors may account for this discrepancy, the most important being the difference of i-graphite sample. Krauss et al. performed their tests on graphite originating from the FRJ-1 (Merlin), whereas the present study uses samples from the TRIGA Mainz. Differences in graphite origin, including impurity content, irradiation history, and microstructure, can therefore reasonably lead to discrepancies between the two datasets. An additional factor being the performance and temperature control of the high-temperature furnace. In the experiments performed by Krauss et al [6], the exact temperature inside the furnace could not be precisely monitored, making it likely that the actual temperature was lower than the setpoint [12]. In contrast, the furnace used in the present study is equipped with a thermocouple connected to the heating system of the furnace and positioned directly above the sample, enabling accurate and stable temperature control throughout the treatment.

2.3.2. Parameters

After establishing and validating the experimental setup, specific operating parameters were defined for the two sets of graphite samples investigated in this study (originating from TRIGA and FRJ-2). The parameter ranges for the TRIGA samples were selected based on the work of Krauss et al. [6]. Since the thermal treatment for the TRIGA samples was performed first, the experience gained was subsequently used to refine the parameter ranges applied to the FRJ-2 samples. These parameters are summarized in Table 2.

Table 2: Summary of the range of tested parameters for thermal treatment of irradiated graphite samples originating from different reactors.

Origin of sample	Relative humidity (%)	Temperature (°C)	Time at T_{max} (h)
TRIGA Mainz	0–5–28.8–50.2–75	1000–1300–1500	2–4
FRJ-2	0–5–15–28.8	1000–1100–1200–1300–1500	2–4–6–8

3. Results and Discussion

3.1. Mass Loss and Structural Results

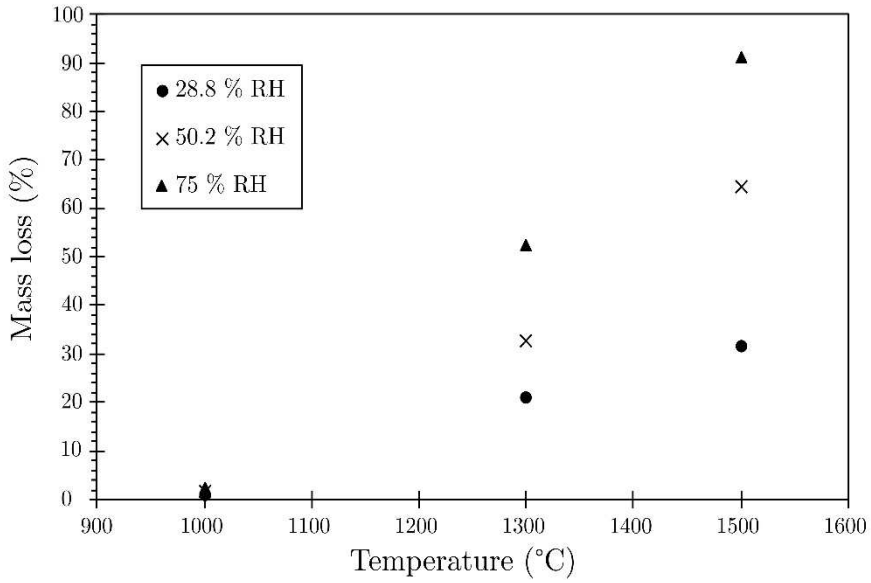

Figure 2: Evolution of the mass loss for i-graphite sample (TRIGA Mainz sample) at different temperature with varying relative humidity (RH).

As part of the characterization, each graphite sample was weighed before and after thermal treatment to determine the corresponding mass loss. As previously discussed, minimizing mass loss is desirable when the goal is to recycle the material. However, when the primary objective is the release of volatile radionuclides, mass loss becomes a secondary consideration. Figure 2 shows the influence of relative humidity and temperature on the mass loss of irradiated graphite samples after 4 h of thermal treatment.

As shown in Figure 2, a clear dependence on both temperature and relative humidity can be observed. Higher values of these parameters lead to increased mass loss, which can be attributed to the more oxidative environment inside the furnace. With rising temperature, the reaction kinetics of graphite oxidation are accelerated, and the higher partial pressure of water vapor enhances the availability of oxidizing species. In this regime, steam can penetrate deeper into the graphite pore network, promoting in-pore oxidation and thereby increasing the overall burn-off.

Additional experiments conducted with a shorter treatment duration of 2 h showed comparable trends, confirming the strong influence of temperature and humidity on oxidation behavior. However, as expected, the overall mass losses were lower after 2 h, reflecting the shorter exposure time and reduced extent of the graphite–steam reaction. Moreover, it is worth mentioning that no direct correlation between the mass loss and the release fraction of ^{3}H and ^{14}C was observed.

Furthermore, samples treated at 1300 °C or above, even at moderate humidity levels, exhibited a marked loss of structural integrity after treatment. This degradation was evident upon visual inspection and handling, as the material readily crumbled under minimal mechanical stress. The combined effects of elevated temperature and steam exposure thus not only intensified oxidation but also contributed to microstructural weakening.

3.2. Release Fraction of Pure Beta Emitters

The following section presents the different release fractions of ^{3}H and ^{14}C in both TRIGA and FRJ-2 samples according to the varying parameters. However, the results for both origins are not compared directly since the irradiated graphite samples possess different impurity levels, origins, and positions within the reactor, etc.

3.2.1. Release Behavior of ^{3}H

The first series of experiments was conducted on samples originating from the TRIGA reactor. Subsequently, the results and expertise obtained from these experiments were used to perform the second set of experiments using irradiated graphite samples originating from the FRJ-2 reactor.

As detailed in Section 2.3.2, several experimental parameters were varied. The first parameter studied was the influence of relative humidity at different treatment temperatures on the release fraction of ^{3}H. The relative humidity ranged from 0 to 75 % for the TRIGA samples, with a temperature range of 1000 to 1500 °C. A narrower relative humidity range of 0 to 28.8 % and a temperature range of 1000 to 1300 °C were tested for the FRJ-2 samples.

The evolution of the release fraction of ^{3}H for both sample origins, (a) TRIGA Mainz and (b) FRJ-2, at varying temperatures and relative humidity values is shown in Figure 3 for a treatment duration of 4 h at the maximum temperature.

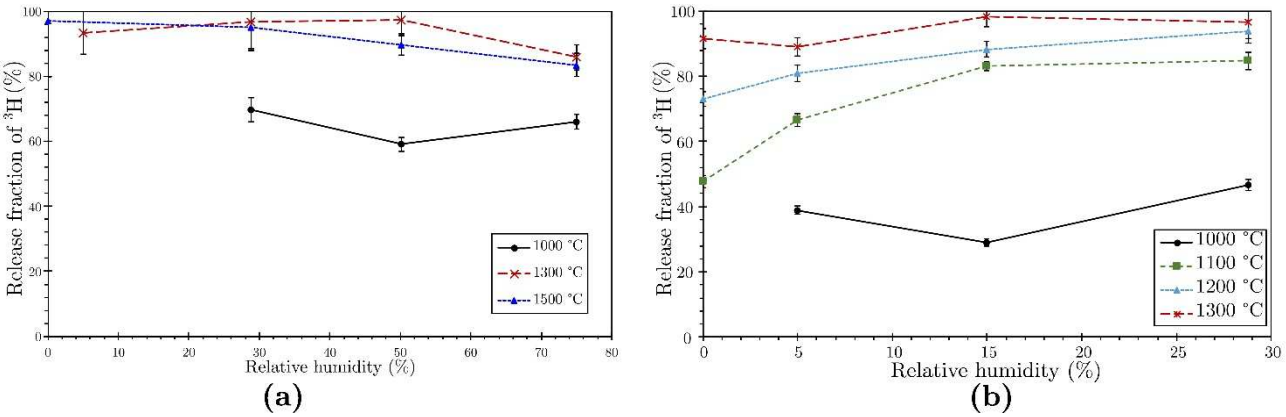

Figure 3: ^{3}H release fraction (%) from a) TRIGA Mainz and b) FRJ-2 graphite samples as a function of relative humidity (%) for various treatment temperatures. Each experiment was conducted for 4 h.

As can be seen in Figure 3(a), the release of ^{3}H in the TRIGA samples is not significantly influenced by the relative humidity and within the uncertainties, the release fraction is almost

constant. Linear trends are observed for each temperature. The release fractions at 1300 °C and 1500 °C are essentially identical, both indicating near-complete removal of ^{3}H under conditions of low or negligible humidity. In contrast, at 1000 °C the tritium release remains incomplete, reaching a maximum of approximately 75 %. Consequently, the subsequent tests conducted on samples from FRJ-2 were carried out at temperatures between 1000 °C and 1300 °C, avoiding higher, energy-intensive temperatures that provided no additional release benefit. The maximum system humidity was maintained at 28.8 % to further limit mass loss and preserve structural integrity. The results of these experiments are presented in Figure 3(b). Similar trends to those observed for the TRIGA samples are evident. The treatment temperature has a stronger influence on the release behavior of ^{3}H than the relative humidity within the system. A slight increase in the release fraction is observed when a small amount of humidity (5 %) is introduced; however, this effect may also be attributed to inherent uncertainties related to the graphite matrix composition and the position of the sample within the reactor prior to treatment.

The results from the previous experiments indicated that nearly complete release of ^{3}H occurs at temperatures of 1300 °C and above. This behavior can be attributed to the temperature dependence of the graphite–steam reaction. As discussed in Section 2.1.2, this reaction occurs within a specific temperature range that is influenced by factors such as sample purity, size, and irradiation history. For the TRIGA Mainz samples, the transition to the second oxidation regime begins between 1000 °C and 1300 °C. For the FRJ-2 samples, this transition is narrowed down to occur between 1000 °C and 1100 °C, allowing improved gas penetration into the pore network and thereby enhancing the decontamination efficiency. The results also showed that the relative humidity within the system does not significantly affect the tritium release fraction but has a strong influence on the sample mass loss, as shown in Section 3.1.

The next parameter investigated was the treatment duration in order to determine whether the release fraction followed a specific evolution over time or if a plateau would be reached after a certain treatment period. Figure 4 presents the release fractions of ^{3}H for the FRJ-2 and TRIGA i-graphite samples, obtained at different temperature and treatment durations at maximum temperature.

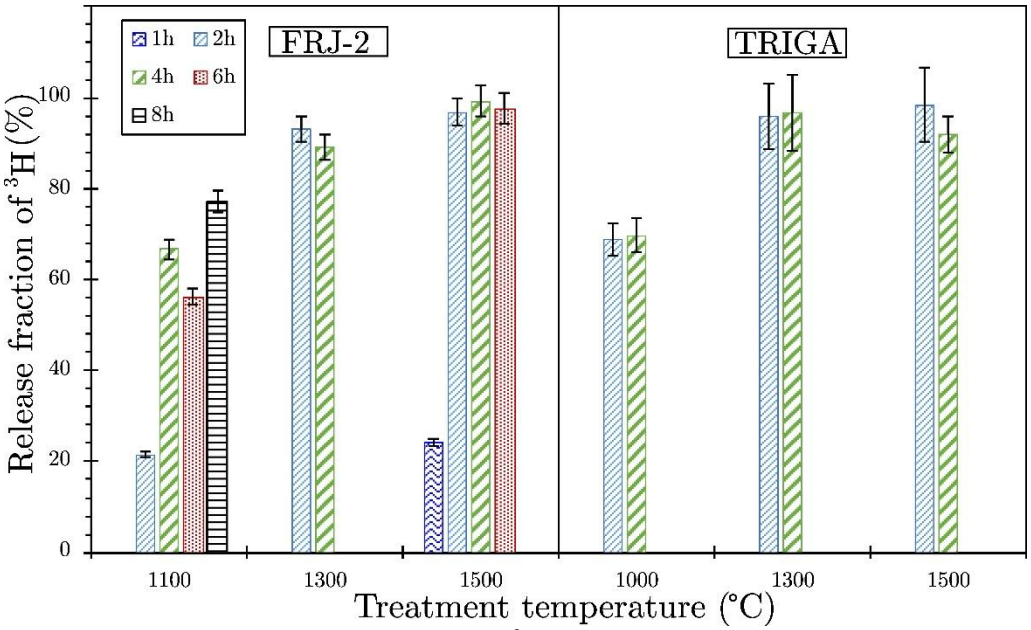

Figure 4: Evolution of the release fraction of ^{3}H at different temperature for varying time of treatment for the FRJ-2 and the TRIGA Mainz i-graphite samples.

The results presented in Figure 4 show that, for the FRJ-2 samples, the treatment temperature influences the time required to reach the maximum release fraction of ^{3}H. At higher temperatures, the plateau is reached after 2 h of treatment, whereas at lower temperatures

(<1300 °C), a treatment duration of approximately 4 h is required to achieve the plateau. For the TRIGA samples, the plateau is reached after 2 h of treatment regardless of the applied temperature. This difference can be explained by several factors, including the graphite matrix and composition, sample size, irradiation duration, and irradiation history.

Overall, these results demonstrate that a treatment duration of 4 h is sufficient to remove the maximum releasable fraction of ^{3}H from irradiated graphite samples under the investigated conditions. Increasing the treatment time up to 8 h does not result in further improvement in the release fraction. Therefore, a treatment duration of 4 h was selected as the optimal condition in order to limit energy consumption while maintaining maximum release efficiency.

Based on the results obtained with the TRIGA and FRJ-2 samples, the most effective conditions for the removal of ^{3}H were achieved at 1300 °C for 4 h with little to no relative humidity, thereby minimizing mass loss and structural degradation.

3.2.2. Release Behavior of ^{14}C

The results for the release of ^{14}C were obtained from the same experiments conducted for ^{3}H. Therefore, the same parameters were investigated, as described in detail in the previous section. The first studied parameter was the time of treatment. Figure 5 presents the evolution of the release fractions of ^{14}C for the i-graphite samples of FRJ-2 and TRIGA at different times of treatment (ranging from 2 h to 8 h) at varying temperatures (1000 °C to 1300 °C).

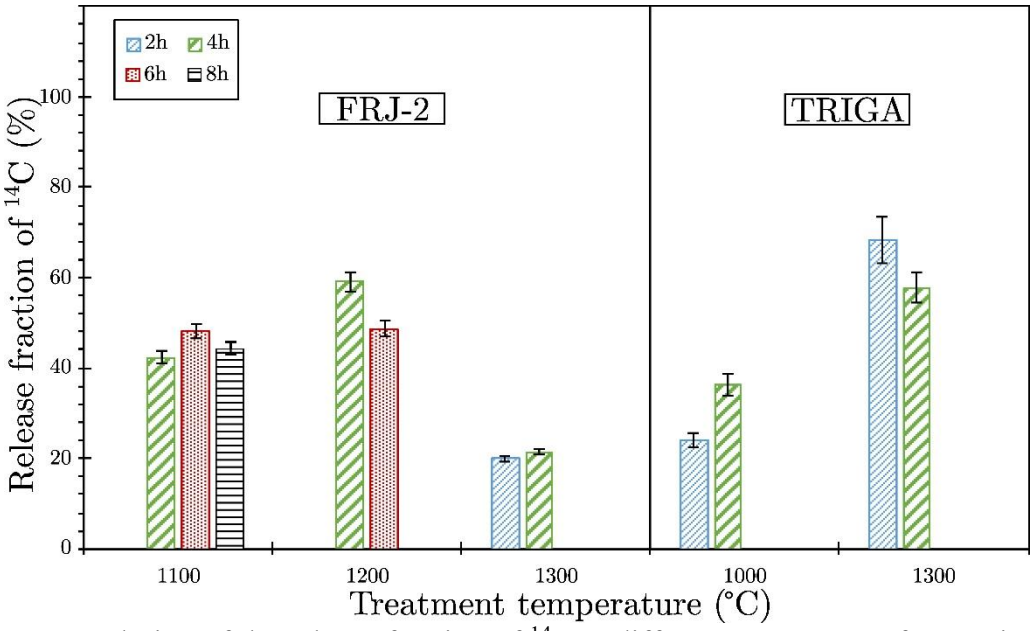

Figure 5: Evolution of the release fraction of ^{14}C at different temperature for varying time of treatment for FRJ-2 and TRIGA Mainz i-graphite samples.

As can be seen in Figure 5, the release fraction of ^{14}C is not significantly influenced by the treatment duration for either the FRJ-2 or the TRIGA samples. The small observed deviations can be attributed to inherent uncertainties related to the graphite matrix, composition, and position within the reactor prior to treatment, among other factors. Overall, these results suggest that extending the treatment duration beyond 2 h does not lead to a notable improvement in the release fraction of ^{14}C. However, since ^{3}H exhibits more efficient removal after 4 h of treatment, this duration was retained as the optimal treatment time, as it is also consistent with the observed ^{14}C release behavior.

The next investigated parameter was the influence of relative humidity at different treatment temperatures. The relative humidity ranged from 0 to 75 % for the TRIGA samples, with a

temperature range of 1000 to 1500 °C. A narrower relative humidity range of 0 to 28.8 % and a temperature range of 1000 to 1300 °C were tested for the FRJ-2 samples. The evolution of the release fraction of ^{14}C for both sample origins, (a) TRIGA Mainz and (b) FRJ-2, at varying temperatures and relative humidity values is shown in Figure 6 for a treatment duration of 4 h at the maximum temperature.

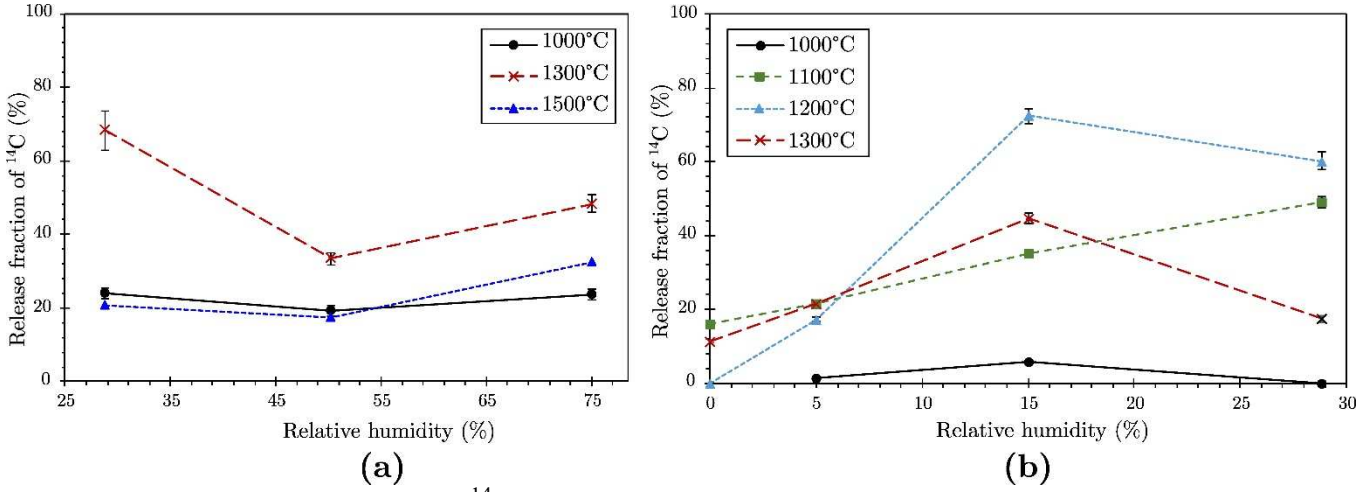

Figure 6: Release fraction of ^{14}C for the (a) TRIGA, (b) FRJ-2 i-graphite samples at varying relative humidity (%) and different temperature of treatment. The treatment was performed for 4h.

As can be seen in Figure 6(a) for the TRIGA samples , the relative humidity inside the system has a strong influence on the release fraction of ^{14}C at 1300 °C. At both lower and higher temperatures, this influence is significantly reduced. Furthermore, a maximum release fraction is observed at moderate relative humidity (28.8 %), followed by a sharp decrease at 50.2 % and a slight re-increase at 75 %. A similar trend is observed for the FRJ-2 samples. It is clear from the different curves that a maximum release fraction, regardless of the temperature, is reached at 15 % relative humidity. The temperature yielding the highest release appears to be 1200 °C. However, it should be noted that under these conditions the sample becomes friable and undergoes significant mass loss (approximately 30 %). The deterioration of the structural integrity becomes even more severe at 1300 °C, with a mass loss of approximately 40 % and complete powderization of the sample. In contrast, at 1100 °C no visible structural degradation is observed and lower mass losses (<10 %) is obtained.

The experimental results for ^{14}C led to conclusions similar to those drawn for ^{3}H. The most effective decontamination of both radionuclides occurs within the temperature range of 1000–1300 °C, with optimal release observed around 1300 °C for the TRIGA samples and around 1100–1200 °C for the FRJ-2 samples, depending on the desired post-treatment form of the sample. This behavior is consistent with the transition from the chemically controlled regime, dominant at 1000 °C, to the in-pore diffusion-controlled regime, where oxidizing species can penetrate the graphite pore network more efficiently. In this regime, the reaction proceeds throughout the internal surface area, thereby enhancing isotope release while still maintaining structural integrity. At higher temperatures, around 1500 °C for the TRIGA samples and 1300 °C for the FRJ-2 samples, the process becomes limited by external mass transfer, leading to accelerated surface corrosion without additional improvement in decontamination efficiency.

- *Influence of Sample Position*

The influence of the sample position within the reactor before the treatment was then investigated for the FRJ-2 samples. The maximum release of ^{14}C for the FRJ-2 samples was actually reached at 1100 °C, with a release fraction of 89 ± 3 %. When replicate experiments

were performed to confirm the observed trend, inconsistencies were noticed despite using identical experimental conditions (the average value of all 19 replicates is used in Figure 6). The only varying parameter in these experiments was the sample origin. As explained in section 2.1.1, the FRJ-2 samples are coming from a single core drill that has been subdivided into five sections. Each section (of 12 cm height) has therefore, a different relative position to the reactor core, with section 1 being the closest and section 5 being the farthest away. Figure 7 presents the release fractions of 14C obtained under identical optimal treatment conditions (1100 °C, 4 h, 15 % relative humidity) for samples taken from each section. A minimum of three replicates

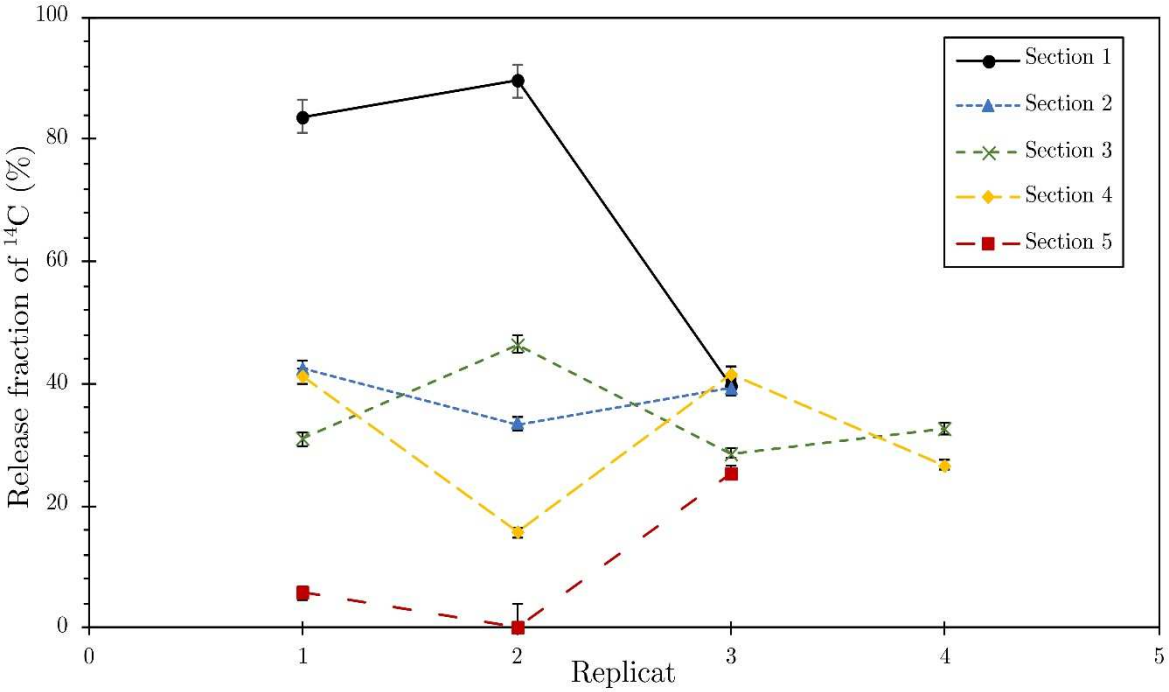

per section was performed to ensure statistical reliability of the results.

Figure 7: Influence of used section on the release fraction of ^{14}C in %. The sections of the i-graphite samples are from the FRJ-2, with section 1 being the closest to the reactor core and 5 the furthest away prior to the treatment. The experiments were performed using the best settings: 1100 °C, 4h, 15 % relative humidity

As can be seen from Figure 7, the release fraction of ^{14}C is heavily influenced by the origin of the sample within the reactor. The relative release of ^{14}C is higher with samples from section 1, located closest to the reactor core. It is observed that the last replicate of this section is lower than the other two. The value is, however, within the range of section 2. The sample could be coming from the border between sections 1 and 2, explaining its close value to the ones from section 2. As each small fragment is coming from a random place within its own cylindrical section of 12 x 15.2 cm. Sections 2 to 4 have a similar average, with section 4 having the most deviation between the different values, which could also be explained by the potential border position of the treated sample. At last, section 5 shows little to no release of ^{14}C. The last replicate would appear to come from the border between sections 4 and 5. The average of the release fraction of ^{14}C and ^{3}H for each section position was thereafter studied at the best settings (1100 °C, 15 % relative humidity, 4 h) and are represented in Figure 8.

Figure 8: Evolution of the relative release fraction of ^{14}C and ^{3}H in % for the FRJ-2 samples according to the position of the samples within the reactor prior to treatment with section 1

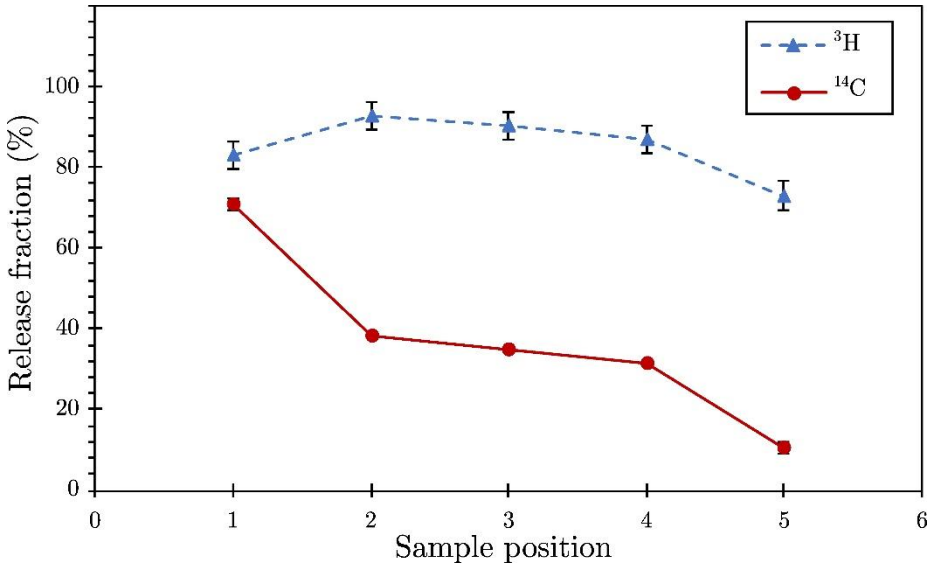

being the closest to the reactor core and 5 the furthest away prior to the treatment. The experiments were performed using the best settings: 1100 °C, 4 h, 15 % relative humidity.

As shown in Figure 8, the release fraction of ^{3}H is almost constant with a plateau between positions 1 to 4. It starts to decrease with a reduction of approximately 15 % at position 5. The influence of sample position is more pronounced for ^{14}C. A clear maximum release fraction of about 70 % is observed for samples originating from position 1, followed by a plateau at approximately 35 % for positions 2 to 4, and a further decrease to around 10 % for position 5.

Overall, both radionuclides exhibit a consistent trend in which samples located farther from the reactor core show lower release fractions after thermal treatment. In addition to relative release fractions, it is also important to consider the absolute release of activity. Figure 9 shows the absolute loss of specific activity (in Bq/g) for both ^{14}C and ^{3}H compared to their initial values before thermal treatment.

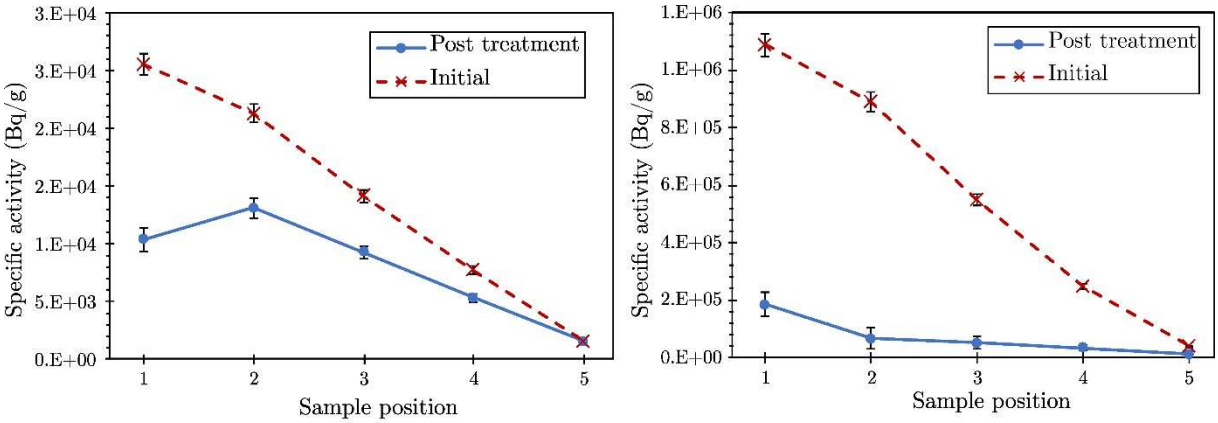

Figure 9: Evolution of the specific activity in Bq/g of a) ^{14}C and b) ^{3}H before treatment and after the treatment according to the position of the samples within the reactor before treatment, with section 1 being the closest to the reactor core and 5 the furthest away prior to the treatment. The experiments were performed using the best settings: 1100 °C, 4 h, 15 % relative humidity.

As shown in Figure 9, both radionuclides exhibit the same trend, where the sample origin strongly influences the post-treatment specific activity. A similar trend is observed for the initial specific activity, which decreases with increasing distance from the reactor core. Samples taken

closer to the core show higher initial activities, resulting in a larger absolute release during treatment.

Additionally, the exhibited trend in which samples located farther from the reactor core show lower release fractions after thermal treatment can also be explained by the irradiation conditions experienced by the different sections. Section 1, located closest to the reactor core, was exposed to a higher neutron flux and consequently underwent more pronounced irradiation damage. Fast neutron irradiation induces damage at both the atomic and crystallographic scales, leading to the formation of local defects and a loss of coherent order, etc. As a consequence, several macroscopic properties of graphite are altered, including porosity, density, thermal conductivity, and mechanical strength. These irradiation-induced modifications increase the accessible reactive surface area, thereby enhancing surface reactivity and facilitating higher reaction rates with oxidizing species [8;14]. Therefore, the release of ^{14}C and ^{3}H in i-graphite samples using thermal treatment under specific conditions is improved.

4. Conclusion and outlook

A substantial removal (>85 %) of both ^{14}C and ^{3}H from irradiated graphite originating from two reactors (FRJ-2 and TRIGA Mainz) was achieved using thermal treatment with steam. After investigating several influencing parameters (duration, temperature of treatment and relative humidity), the best settings were found to be slightly different according to the sample origin and its size. For small samples of approximately 75 mg, the most favorable conditions were identified at 1100 °C for a treatment duration of 4 h, and a relative humidity of 15 %. Under these conditions, removal efficiencies of up to 85 % for ^{14}C and approximately 90 % for ^{3}H were obtained while keeping the structural degradation as little as possible. The release behavior of ^{14}C was found to be strongly influenced by the original position of the graphite within the reactor core, with higher relative release fractions observed for samples located closer to the core, consistent with increased irradiation damage.

Future work will focus on applying the optimized conditions identified in this study to i-graphite samples from additional reactor types, with the aim of refining the operational parameter range and developing a more universal decontamination approach applicable to a variety of i-graphite materials. In addition, scale-up experiments will be conducted to assess the feasibility of transferring the process to larger sample masses and adapting the settings to bigger samples.

This study focuses on the removal of ^{14}C and ^{3}H from irradiated graphite samples. Complementing this work, the high-temperature removal of gamma-emitters such ^{60}Co, ^{133}Ba,^{137}Cs, $^{152,154,155}Eu$ and ^{241}Am was evaluated by Meunier et al. [15]. To streamline the decontamination process, an integrated approach combining the optimal conditions for both radionuclide groups was tested using temperature, time, and relative humidity gradients. This combined method successfully achieved the maximum release rates for all radionuclides reported here and in [15].

Furthermore, within the scope of the i-GraDe project, Supercritical Fluid Extraction (SCFE) is being explored as an alternative decontamination pathway [16]. Preliminary experiments coupling thermal treatment with SCFE have been performed and are currently under evaluation.

5. Acknowledgment

This project was funded by the Federal Ministry of Research, Technology and Space (BMFTR) of Germany, under grant number 15S9442. We thank Ch. E. Düllmann for his support of our work. We would also like to acknowledge the team from the TRIGA Mainz and from JEN

(Jülicher Entsorgungsgesellschaft für Nuklearanlagen) for providing us with samples and valuable information.

References

[1] J. Fachinger, W. von Lensa, and T. Podruzhina, "Decontamination of nuclear graphite," *Nuclear Engineering and Design*, vol. 238, no. 11, pp. 3086–3091, 2008.

[2] IAEA, *Processing of Irradiated Graphite to Meet Acceptance Criteria for Waste Disposal*, IAEA-TECDOC No. 1790, Vienna, 2016.

[3] L. Kuhne, C. Rizzato, K. Baginski, N. Trigubowitsch, E. Petrova, D.Vulpius, R. Nabbi, A.Neumann, H-J. Steinmetz, W. von Lensa Entsorgung von betrahltem Graphit (CarboDISP), Final report, (2015).

[4] A. Räty and P. Kotiluoto, "FRJ-1 TRIGA activity inventories for decommissioning planning," *Nuclear Technology*, vol. 194, pp. 28–38, 2016.

[5] N. Heiss, L. Meunier, L. Lens, M. Knebel, and U. W. Scherer, "Irradiated Reactor Graphite: Experimental Characterization – Insights from German Research Reactors," *in press*, *Radiochimica Acta*, 2026.

[6] B. Krauss, *Determination of Decontamination Factors of Irradiated Nuclear Graphite by Steam Reforming*, Jülich, 2013.

[7] T. Podruzhina, *Graphite as Radioactive Waste: Corrosion Behaviour under Final Repository Conditions and Thermal Treatment*, PhD thesis, Aachen University, 2004.

[8] C. Contescu and R. Paul, *Oxidation Behavior and Property Degradation of Nuclear Graphites*, ORNL/TM-2022/1839, 2022.

[9] D. Feron (Ed.), *Nuclear Corrosion Science and Engineering*, Woodhead Publishing Series in Energy, Woodhead Publishing, 2012, Chapter 9, pp. 755–759.

[10] H. Hissen *et al*., "Oxidation experiments and theoretical examinations on graphite materials relevant for the PBMR," *Nuclear Engineering and Design*, vol. 238, pp. 3018–3025, 2008.

[11] DIN EN ISO 11929-1:2021-11, *Bestimmung der charakteristischen Grenzen (Erkennungsgrenze, Nachweisgrenze und Grenzen des Überdeckungsintervalls) bei Messungen ionisierender Strahlung – Grundlagen und Anwendungen – Teil 1: Elementare Anwendungen*, 2019.

[12] U. W. Scherer, private communication.

[13] B. Abdolla, *Dekontamination von bestrahltem Grafit durch oxidative Behandlung in einem Hochtemperaturofen*, Master's thesis, Technische Hochschule Mannheim, Mannheim, 2025.

[14] E. Narkūnas, P. Poškas, A. Šmaižys, and G. Poškas, "Characterization of the Ignalina NPP RBMK-1500 reactor graphite: Review and summary of current situation and recent developments with respect to reactor core dismantlement," *Progress in Nuclear Energy*, vol. 186, article 105805, 2025.

[15] L. Meunier, N. Heiss, L. Lens, B. Abdolla, E. Varkey and U. W. Scherer, "Thermal decontamination of FRJ-2 irradiated graphite: Selective removal of γ-emitting radionuclides," *submitted*, 2026.

[16] N. Heiss, L. Meunier, L. Lens, S. Goedert and U. W. Scherer, “Irradiated Reactor Graphite: Exploring Supercritical Fluid Extraction for the Decontamination of Legacy Material,” *in preparation*, 2026.